

# NORMAL CONDUCTING OPTIONS FOR THE UK'S NEW LIGHT SOURCE PROJECT

C. Christou, R. Bartolini, J.-H. Han, H. Huang and J. Kay  
Diamond Light Source, Oxfordshire, UK

## Abstract

This paper considers the design of a normal-conducting linac FEL in the context of the UK's New Light Source project. Capabilities and limitations of this approach are illustrated by reference to a 3 GeV S-band linac design. The effects of high repetition rate operation and RF jitter are considered.

## THE NEW LIGHT SOURCE PROJECT

The UK's New Light Source (NLS) project [1] was launched in April 2008 to consider the scientific case and develop a conceptual design for a possible next generation light source. The outline facility design will be agreed by January 2009 following consultation with the user community throughout 2008 after which a design report and proposal for funding will be prepared for submission in October 2009.

A high (> 400 Hz) repetition rate of single pulses demands superconducting linac technology operating in continuous-wave. Normal conducting linac technology is however significantly cheaper, allowing a higher energy to be reached for a given cost. Design studies are ongoing for both normal conducting and superconducting linacs. This paper reviews the options for a normal conducting NLS design; a companion paper reviews the superconducting approach [2].

## LINAC LIGHT SOURCE PROJECTS

There has been much recent interest in the use of normal conducting technology for linac FELs. Most projects in construction or development use the well-proven S-band technology used at SLAC for several decades whereas SCSS exploits C-band technology developed in the JLC(C) programme. LCLS and SCSS are scheduled for completion in 2009 [3] and 2011 [4] respectively. The study presented here considers an S-band linac for NLS, although X-band technology has not been ruled out, particularly considering possible technology developments following the decision to change the CLIC design frequency to 12 GHz [5].

## NORMAL CONDUCTING TECHNOLOGY

Virtually all high-power klystrons operating today are driven by line-type modulators using a reactive pulse forming network (PFN) and a thyatron switch. The line-type modulator can be the dominant cost driver in a linac [6]. The self-terminating nature of the line-type discharge limits the modulator operation: the pulse length can only be changed by switching the connections to multiple PFNs, and the trailing edge of the pulse is usually not sharp since it depends on the discharge of multiple

reactive elements. The modulator cannot drive loads of different impedances, and the thyatron has a limited operational lifetime. The overall efficiency of a line-type modulator is as low as 50% to 60% and the thyatron is a single-point of failure of the modulator.

An approach that would mitigate many of these problems in NLS is the use of an Insulated Gate Bipolar Transistor (IGBT) switch together with a solid state induction modulator: this is a stack of small pulse transformers in which the primaries of the cores are driven in parallel by separate sets of IGBT switches and capacitors operated at relatively low voltage (2-4kV). The high voltage is developed at the secondary in series [7].

Repetition rate of a line type modulator and klystron is limited by modulator charging rate or thyatron recovery time. Incorporation of an IGBT switch increases the available repetition rate from the modulator and power dissipation in the klystron is then the limiting factor.

Table 1: High Power Klystrons of Interest to NLS

Manufacturer	Thales	Toshiba	SLAC
Model	TH2155	E3730A	XL4
Waveband	S-band	S-band	X-band
Frequency	2998 MHz	2856 MHz	11.42 GHz
Peak power	45 MW	50 MW	50 MW
Efficiency	44%	45%	40%
Gain	54 dB	51 dB	50 dB
Pulse length	3.5 $\mu$ s	4 $\mu$ s	1.5 $\mu$ s

Table 1 shows high power klystrons available in S-band and X-band. S-band klystrons already exist that separately satisfy high average and high peak power demands. The enhanced collector cooling that is provided in the former needs to be combined with a high peak power klystron, and manufacturers have indicated their readiness to supply this; repetition rates of up to 400 Hz are envisaged. A redesign of the klystron gun to reduce the arcing rate is also being discussed.

Table 2: Comparison of the DESY Type II Linac and SLAC 3 m Accelerating Structures available at 2998 MHz

Property	DESY structure	SLAC structure
Length	5.2 m	3.0 m
Shunt impedance	51.5 M $\Omega$ /m	52 M $\Omega$ /m
Attenuation	0.5 Neper	0.49 Neper
Mode	$2\pi/3$	$2\pi/3$
Q	14000	12500
Filling time	740 ns	690 ns
Number of cells	156	89

The two main types of S-band accelerating structure that are readily available are the DESY type II and SLAC 3 m ones; these structures are compared in Table 2.

Performance of the structures is similar, and the 3 GeV NLS requirements can be met by either design with an accelerating gradient of around 20 MV/m.

The power delivered by the klystron can be compressed with a SLED cavity. Figure 1 shows the increase in acceleration through a DESY structure achievable with a SLED cavity with  $Q_0=10^5$  and  $\beta=6.7$ , together with power dissipation in a single pulse.

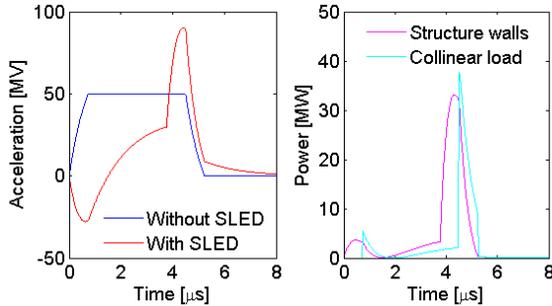


Figure 1: Acceleration through a DESY structure with and without SLED (left) and powers dissipated in structure and collinear load in a single pulse with SLED (right).

400 Hz repetition rate at 20 MV/m is much higher than operating rates of 120 Hz at SLAC and 50 Hz at DESY for similar gradients. At this rate, average klystron power is 70 kW. Average power dissipation limits have not been explored for either structure or for SLED cavities, and further work is required to determine what repetition rate is achievable. As a first estimate of the capability of an S-band structure to withstand such power levels, a thermal model has been developed. SUPERFISH was used to solve for the two accelerating modes in a 3 GHz structure, based on an adaptation of the SLAC 2856 MHz design, and shown in Figure 2 (dimensions in inches). Power transfer at the walls for these two modes was then taken as an input for a thermal model shown in Figure 3, demonstrating that with suitable water cooling on the outer surface of the structure, the temperature of a normal cell can be kept at an average of 30°C to 35°C.

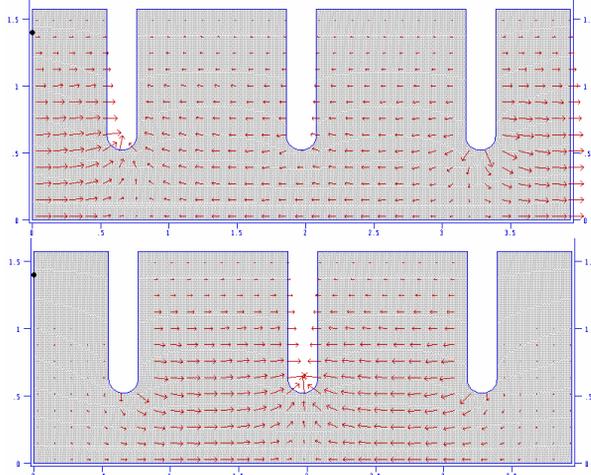


Figure 2: Accelerating modes in an S-band structure.

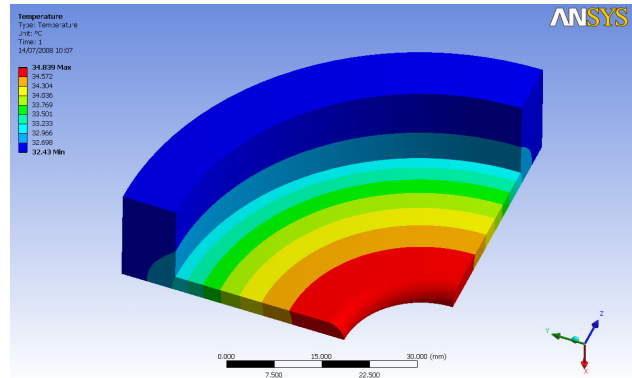


Figure 3: Equilibrium temperatures in an S-band structure operating at 400 Hz: blue is 32.4°C, red is 34.8°C.

The main design difference between the DESY and SLAC structures is the use of a collinear load in the DESY structure and an external load in the SLAC structures. While the DESY approach preserves the symmetry of the structure, it may prove to be more difficult to adapt the cooling to cope with the high power dissipated in the collinear load, as 38% of the total power must be dissipated in the final 8 cells of the structure. A full thermal model of the whole structure is needed before the impact of the intense heating can be fully assessed, but problems may arise in the matching of the load to the main part of the structure because of the existence of a longitudinal temperature gradient. Rapid thermal cycling of the load cells may also be problematic, as the SLED cavity delivers a very high power pulse to the load, as shown in Figure 1 and the cyclic stress may lead to metal fatigue. For fully annealed OFE copper the temperature rise required to initiate fatigue stress has been measured to be between 40 K [8] and 110 K [9]. Heat dissipation in the resistive coating in the load cells is a particular point of concern. We have therefore provisionally selected the SLAC structure for beam dynamics simulations and layout considerations.

## LINAC BEAM DYNAMICS

A suitable NLS 3 GeV design consists of 12 RF stations operating at 2998 MHz, each driving up to 4 SLAC structures, plus one X-band linearising structure, two bunch compressors (at 460 MeV and 1.2 GeV) and one dog-leg immediately before the undulator section. The beam dynamics in the linac have been calculated with ELEGANT, taking CSR and wakefields into account [10]. Input is from an ASTRA model of a new S-band gun [11]. Initial simulations have been carried out with a charge of 0.2 nC, showing that the linac can deliver a 3 GeV beam with of peak current 7 kA, 0.7 mm mrad normalised emittance and 0.2% energy spread [12].

The sensitivity of the linac to jitter in RF phase and accelerating gradient of the structures has been studied in order to generate a baseline specification for modulator stability and low-level RF. This first stage analysis considers beam at the exit of the linac.

Figure 4 shows the change of peak linac current for a one percent change in gradient at all RF stations along the linac including the X-band structure. The first S-band plant is considered part of the injector and so is not studied here. Sensitivity is highest for RF stations S2 and S3 before BC1, smaller for S4 to S6 between the bunch compressors and smaller again after BC2.

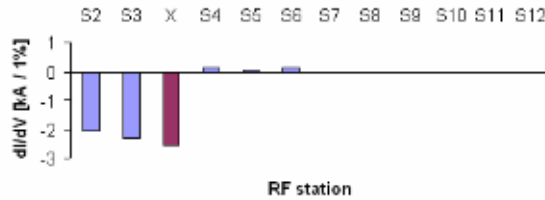


Figure 4: Sensitivity of peak beam current to accelerating gradient for all RF stations.

More detailed study of station S2 shown in Figure 5 shows the effect of changes in gradient, or accelerating voltage, on emittance. Large phase changes affect the bunch compression such that the peak beam current increases rapidly to tens of kA and horizontal emittance blows up through CSR effects. The figure shows perturbation of  $\pm 5\%$  and  $\pm 5^\circ$  about the working point.

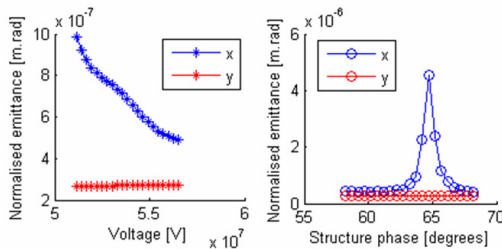


Figure 5: Output pulse emittance as a function of voltage and phase in the first accelerating structure.

The sensitivity of the different RF stations to small changes in RF voltage and phase are summarised in Table 3. In general, effects are greatest on the X-band structure and before the first bunch compressor.

Table 3: Sensitivity of Individual RF Stations to RF Errors

	Before BC1	BC1-BC2	After BC2	X-band	Units
dE/dV	1.64	2.44	3.03	-0.30	MeV/1%
dE/dφ	-0.43	1.81	0.038	1.245	MeV/1°
dε <sub>nx</sub> /dV	-0.076	0.01	4e-4	-0.04	mm.mrad/1%
dε <sub>nx</sub> /dφ	0.87	0.08	2e-4	-0.61	mm.mrad/1°
dI/dV	-2.18	0.11	-7e-3	-2.56	kA/1%
dI/dφ	19.7	1.77	0.055	-12.3	kA/1°

Summaries of the distributions of 10000-particle runs through the ELEGANT model with up to 500 runs at each point are shown in Figure 6. This demonstrates how the beam jitter grows with RF jitter. For comparison, the rms energy of a single 100000 particle distribution with no jitter is 7.0 MeV and the rms in arrival time is 28 fs. Jitter of 0.5° in S-band phase and 0.4% in accelerating structure gradient leads to a 0.1% jitter in beam energy.

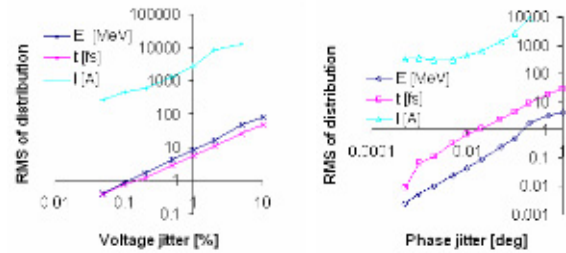


Figure 6: RMS values of mean energy, arrival time and peak current with voltage and phase jitter as displayed.

Similarly, the effect of small physical displacements on the RF structures can be calculated by inserting a lateral displacement or by introducing a kick into the lattice in ELEGANT. Results are summarised in Table 4.

Table 4: Sensitivity of RF Structures to Positioning Errors

	Before BC1	BC1-BC2	After BC2	X-band	Units
dE/dx	9e-3	-0.01	4e-4	0.29	MeV/mm
dε <sub>nx</sub> /dx	-8e-3	7e-3	2e-3	-1.13	mm.mrad/mm
dI/dx	0.46	1.36	1.76	-1.5	kA/mm
dE/dα <sub>x</sub>	-2.39	0.47	2e-3	0.48	MeV/mrad
dε <sub>nx</sub> /dα <sub>x</sub>	1.63	-0.64	0.44	0.27	mm.mrad/mrad
dI/dα <sub>x</sub>	6.53	-8.66	1.10	3.42	kA/mrad

Positioning errors of the X-band structure have a large effect on the beam. For this reason, the X-band structures in the NLC design were designed to be mounted on moveable supports to align with the beam; this approach is recommended for the NLS.

## SUMMARY

Recent advances in solid state modulators, together with the adoption of well proven S-band linac technology offer the prospect of a reliable, cost effective normal conducting linac FEL for the UK New Light Source project operating at repetition rates previously impossible for such an approach. A 3 GeV linac design has been developed and the issues of power dissipation and RF stability have been considered.

## REFERENCES

- [1] <http://www.newlightsource.org/>
- [2] P. A. McIntosh et al, this conference.
- [3] J. N. Galayda, EPAC 08, Genoa, p1939.
- [4] T. Shintake, EPAC 08, Genoa, p136.
- [5] G. Geschonke, EPAC 08, Genoa, p2912.
- [6] ILC Technical Review Committee 2nd Report (2003).
- [7] R. L. Cassel et al, PAC 01, Chicago, p3744.
- [8] D. P. Pritzkau et al, SLAC-PUB-8013 (1998).
- [9] O. A. Nezhevenko, PAC 97, Vancouver, p3013.
- [10] We gratefully acknowledge the initial work carried out on the S-band design optimisation by Y. J. Kim.
- [11] J.-H. Han, this conference.
- [12] R. P. Walker et al, EPAC 08, Genoa, p142.